A New Model for Radical Desorption in Emulsion Polymerization

José M. Asua

Institute for Polymer Materials (POLYMAT) and Grupo de Ingeniería Química, Facultad de Ciencias Químicas, The University of the Basque Country, Apdo. 1072, 20018 Donostia-San Sebastián, Spain

Received April 23, 2003; Revised Manuscript Received June 5, 2003

ABSTRACT: A new first principles model for radical desorption in emulsion polymerization was developed. It was demonstrated that the previous models were erroneous. The new model predicts unexpected dependences of the radical desorption rate coefficient upon the number of polymer particles, particle size, and initiator type and concentration. This may be the reason previous kinetic analysis based on extensive experimental designs were not conclusive in terms of the elucidation of the mechanisms of radical exit. A practical consequence is that the desorption rate coefficients determined under some given experimental conditions cannot be directly used to predict the behavior of emulsion polymerization systems under different conditions.

Introduction

Emulsion polymerization is used in the production of a wide range of specialty polymers including adhesives, paints, binders for nonwoven fabrics, additives for paper, textiles, and construction materials, impact modifiers for plastic matrices, diagnostic tests, and drug delivery systems.[1] The range of products achievable has expanded due to the development of miniemulsion polymerization[2−4] and to the implementation of controlled radical polymerization in dispersed media.[5,6]

From a mechanistic point of view, radical compartmentalization is likely the most distinctive feature of emulsion polymerization. This refers to the fact that the radicals are distributed among the different particles, and hence, radicals in different particles cannot terminate between them. This allows one to simultaneously achieve high polymerization rates and high molecular weights. Both the polymerization rate and the molecular weights depend on the number of radicals per particle, which in turn depends on the relative rates of radical entry from the aqueous phase, radical exit from the polymer particles, and bimolecular termination in the polymer particles. Therefore, there is strong interest in developing predictive models for these processes.

Radical desorption occurs upon formation of a single-unit radicals by chain transfer to monomer or to chain transfer agents (CTA) followed by diffusion of the newly formed radical to the aqueous phase. Radical desorption is commonly accounted for by the desorption rate coefficient, k_d, such as the overall rate of radical desorption for a population of N_p polymer particles with an average number of radicals per particle, $\tilde{n}$, is $R_{exit} = k_d \tilde{n} N_p$ (radicals/L·s). This is a convenient way of modeling radical exit because it allows solving the population balances of particles containing n radicals with a moderate mathematical effort.

Nomura[7] and Asua et al.[8] developed different equations for k_d resulting from a different way of considering the reabsorption of the desorbed radicals. Nomura[7] considered irreversible entry of the reabsorbed radicals, whereas Asua et al.[8] took into account the possibility of redesorption. Asua et al.[8] were able to explain experimental results[9] that Nomura's model could not justify. More recently, Casey et al.,[10] claiming that the previous models did not take properly into account the differences between initiator-derived radicals and monomeric radicals, proposed a detailed and rather lengthy model for radical desorption. However, it has been demonstrated[11] that this model is mathematically equivalent to the model proposed by Asua et al.,[8] whose simpler mathematical form presents practical advantages.

Despite the apparent advantages of the model proposed by Asua et al.,[8] in the first part of the present work, it is demonstrated that such a model does not account properly for the fate of the desorbed radicals, which may have severe consequences on the predictions of the radical exit, and consequently on the predictions of polymerization rate and molecular weights. In the second part of this article, a new model for radical desorption based on first principles is developed.

Analysis of the Previous Model

Let us consider the case in which the single-unit radicals are formed by chain transfer to monomer. Under these circumstances, the rate coefficient for radical exit derived by Asua et al.[8] was as follows:

$$k_d = k_{fm}[M]_p \frac{K_o}{\beta K_o + k_p[M]_p} \ (s^{-1}) \qquad (1)$$

where k_{fm} is the rate coefficient for chain transfer to monomer, $[M]_p$ the monomer concentration in the polymer particles, K_o the rate of diffusion of the monomeric radical out of the particle, k_p the propagation rate constant, and β the probability that the monomeric radical reacts in the aqueous phase by either propagation or termination.

When all the desorbed radicals react in the aqueous phase, $\beta = 1$, and eq 1 approaches

$$k_d = k_{fm}[M]_p \frac{K_o}{K_o + k_p[M]_p} \ (s^{-1}) \qquad (2)$$

Equation 2 establishes that the exit rate is the rate of production of monomeric radicals in the polymer particle times the probability of desorption of these radicals, which seems to be a reasonable limit of the general equation.

10.1021/ma0345192 CCC: $25.00
Published on Web 07/11/2003

On the other hand, when the reactions of the desorbed radicals in the aqueous phase are negligible, $\beta = 0$, and eq 1 approaches

$$k_d = k_{fm}[M]_p \frac{K_o}{k_p[M]_p} \ (s^{-1}) \tag{3}$$

Equation 3 predicts a positive value of k_d when $\beta = 0$. However, $\beta = 0$ means that all of the desorbed radicals reenter the polymer particles, and under these circumstances, the net rate of radical exit is zero. This is a proof that the desorption rate coefficient derived by Asua et al.[8] is erroneous. As shown in Appendix I, the origin of the error is that Asua et al.[8] did not account properly for the fate of the desorbed radicals. In Appendix I, instead of detailing the errors involved in the derivation of eq 1, an upgraded derivation of k_d is presented following a method similar to that used in the development of eq 1. It is worth pointing out that this only leads to an approximate equation for k_d. Therefore, in the next section a first principles rigorous model for the rate coefficient for radical exit is presented.

First Principles Desorption Rate Coefficient

Let us consider the population of polymer particles containing n radicals. This population is composed by a large number of particles (typically in the range of 10^{17} particles/L). Considering one of these particles, a monomeric radical formed in such a particle by chain transfer to monomer (formation of single-unit radicals by chain transfer to CTA can be readily included in this approach) will perform a diffusive random walk through the amorphous structure of the monomer swollen polymer particle until it either reacts in the polymer particle (by either propagation or termination) or desorbs from the polymer particle. Similar processes occur in all particles containing n radicals. In practice, one cannot handle the information associated with each of the individual trajectories of the monomeric radicals in every polymer particle, and some kind of average is needed. This average is given by the behavior of a single polymer particle representative of the population of polymer particles with n radicals.

To develop the equations describing the behavior of the representative particle, let us consider the similarity between the present case and the Monte Carlo simulations carried out to model the diffusion of small molecules in polymers. In these simulations, the diffusion paths of a series of small molecules are computed and then averaged to estimate a Fickian diffusion rate coefficient. In the present case, the trajectory of each monomeric radical is the equivalent to one of the Monte Carlo paths; therefore, the average of all the trajectories results in a concentration profile of monomeric radicals (such as that illustrated in Figure 1), which can be modeled using a Fickian equation. This concentration profile depends on the relative rates of generation, diffusion, propagation, and termination of monomeric radicals in the polymer particles and on the resistances offered by the hairy layer formed by the steric surfactant (if present) and by the stagnant liquid film around the polymer particle.

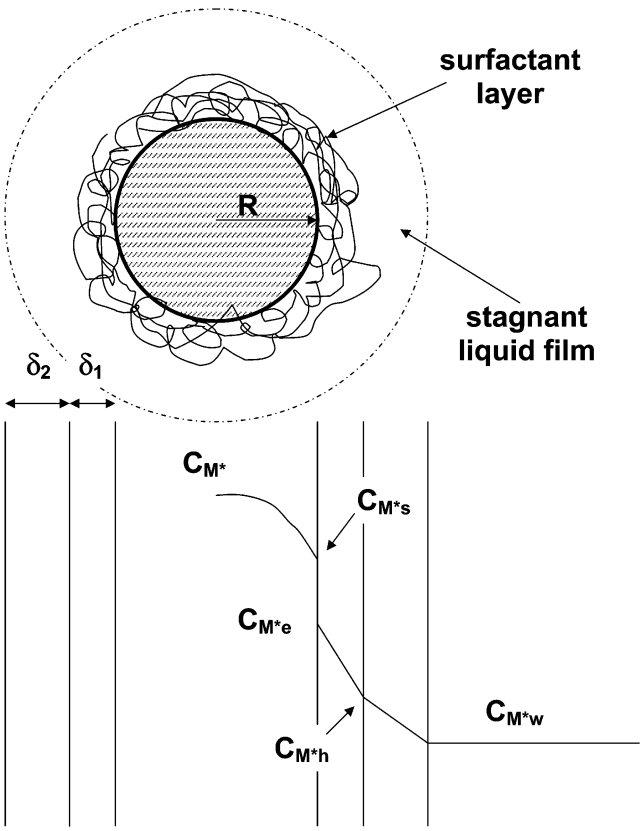

Figure 1. Monomeric radical concentration profiles.

Under steady-state conditions, the material balance of monomeric radicals in polymer particles containing n radicals is

$$D_p \frac{1}{r^2} \frac{d\left(r^2 \frac{dC_{M^*}}{dr}\right)}{dr} + k_{fm}[M]_p \frac{n}{v_p N_A} = \left(k_p[M]_p + 2k_t \frac{n-1}{v_p N_A}\right) C_{M^*} \tag{4}$$

where D_p is the diffusion rate coefficient in the polymer particles, C_{M^*} the concentration of monomeric radicals in the polymer particles, v_p the volume of the polymer particle, N_A the Avogadro number, and k_t the termination rate constant in the polymer particles. In eq 4, it was assumed that the concentration of long-chain radicals was homogeneous through the polymer particles, namely, that there was no radical concentration profiles resulting from the surface anchoring effect. The case in which there is a radical concentration profile is summarized in Appendix II.

Equation 4 can be integrated analytically giving the following concentration profile of monomeric radicals

$$\frac{C_{M^*}}{C_{M^*s}} = \frac{R}{r}\left(1 - \frac{\gamma n}{\eta}\right)\frac{\sinh(r\sqrt{\eta})}{\sinh(R\sqrt{\eta})} + \frac{\gamma n}{\eta} \tag{5}$$

where C_{M^*s} is the concentration of monomeric radicals

at the surface of the polymer particles (see Figure 1), and

$$\gamma = \left(k_{fm}[M]_p \frac{1}{v_p N_A}\right)/D_p \quad (6)$$

$$\eta = \left(k_p[M]_p + 2k_t \frac{n-1}{v_p N_A}\right)/D_p \quad (7)$$

It is worth pointing out that under most conditions $k_p[M]_p \gg k_t(n-1)/v_p N_A$, and hence eq 7 reduces to

$$\eta = k_p[M]_p/D_p \quad (8)$$

The rate of radical exit from one polymer particle is as follows:

$$R_{exit1}(n) = 4\pi R^2 D_p\left(-\frac{dC_{M^*}}{dr}\right)_{r=R} = 4\pi R D_p (R\sqrt{\eta}\coth R\sqrt{\eta} - 1)\left[\frac{\gamma n}{\eta} - C_{M^*s}\right] \text{(mol/s·particle)} \quad (9)$$

Similarly, the material balance for monomeric radicals in the hairy layer surrounding the polymer particle led to the following rate of exit of monomeric radicals through the hairy layer:

$$R_{exit2}(n) = 4\pi R \frac{(R+\delta_1)}{\delta_1} D_h (C_{M^*e} - C_{M^*h}) \text{ (mol/s·particle)} \quad (10)$$

where δ_1 is the thickness of the hairy layer, D_h is the diffusion rate coefficient in the hairy layer, C_{M^*h} is the concentration of monomeric radicals at the interface between the hairy layer and the aqueous phase, and C_{M^*e} is related to the concentration of monomeric radicals at the surface of the polymer particles by means of a partition coefficient, m

$$C_{M^*s} = m C_{M^*e} \quad (11)$$

The material balance in the stagnant layer surrounding the polymer particle led to the rate of exiting monomeric radicals going through this layer

$$R_{exit3}(n) = 4\pi(R+\delta_1)\frac{(R+\delta_1+\delta_2)}{\delta_2} D_w (C_{M^*h} - C_{M^*w}) \text{ (mol/s·particle)} \quad (12)$$

where δ_2 is the thickness of the stagnant liquid film, D_w the diffusion rate coefficient in the aqueous phase and C_{M^*w} the concentration of monomeric radicals in the aqueous phase.

Under steady-state conditions, $R_{exit} = R_{exit1} = R_{exit2} = R_{exit3}$, and combination of eqs 9−12 yields the following equation for the rate of exit

$$R_{exit}(n) = [4\pi D_w(R+\delta_1)(R+\delta_1+\delta_2)/\delta_2]/\left[1 + \frac{D_w}{D_h}\times\frac{(R+\delta_1+\delta_2)\delta_1}{R\delta_2} + \frac{D_w}{D_p m}\frac{(R+\delta_1)(R+\delta_1+\delta_2)}{R\delta_2}\times\frac{1}{R\sqrt{\eta}\coth R\sqrt{\eta} - 1}\right]\left(\frac{\gamma n}{\eta m} - C_{M^*w}\right) \text{ (mol/s·particle)} \quad (13)$$

It is believed that, at least for dilute latexes, the thickness of the stationary layer δ_2 is much larger than the particle size[12] (some indirect proof is provided in Appendix III). On the other hand, the thickness of the hairy layer is expected to be small as compared with the particle size. For $\delta_2 \gg R$ and $R \gg \delta_1$, eq 11 simplifies to

$$R_{exit}(n) = \lambda\left(\frac{\gamma n}{\eta m} - C_{M^*w}\right) \text{ (mol/s·particle)} \quad (14)$$

where

$$\lambda = \frac{4\pi D_w R}{1 + \frac{D_w}{D_h}\frac{\delta_1}{R} + \frac{D_w}{D_p m}\frac{1}{R\sqrt{\eta}\coth R\sqrt{\eta} - 1}} \quad (15)$$

Equation 14 contains the concentration of monomeric radicals in the aqueous phase, which can be obtained from the material balance for the monomeric radicals in the aqueous phase:

$$R_{exit} = (k_p[M]_w + 2k_{tw}[R]_w)C_{M^*w} \text{ (mol/L·s)} \quad (16)$$

where R_{exit} is the overall rate of radical exit given by

$$R_{exit} = \sum_{n=1}^{n=\infty} R_{exit}(n)N(n) = \frac{\lambda\gamma}{\eta m}\tilde{n}N_p - \lambda C_{M^*w}N_p \text{ (mol/L·s)} \quad (17)$$

Combination of eqs 14, 16, and 17 yield the following equation for the overall rate of radical exit:

$$R_{exit} = \lambda\frac{\gamma N_A}{\eta m}\left(1 - \frac{\lambda N_p}{\lambda N_p + k_p[M]_w + 2k_{tw}[R]_w}\right)\tilde{n}N_p \text{ (radicals/L·s)} \quad (18)$$

Therefore, the desorption rate coefficient is

$$k_d = \lambda\frac{\gamma N_A}{\eta m}\left(1 - \frac{\lambda N_p}{\lambda N_p + k_p[M]_w + 2k_{tw}[R]_w}\right) (s^{-1}) \quad (19)$$

Equation 19 shows that, in contrast with what has been previously published in the literature,[7,8] the rate coefficient for radical exit heavily depends on the events in the aqueous phase. Thus, when all of the desorbed monomeric radicals react in the aqueous phase, namely, $k_p[M]_w + 2k_{tw}[R]_w \gg \lambda N_p$ and eq 19 reduces to

$$k_d = \lambda\frac{\gamma N_A}{\eta m} (s^{-1}) \quad (20)$$

On the other hand, when none of the desorbed radicals react in the aqueous phase, namely, $k_p[M]_w + 2k_t[R]_w \ll \lambda N_p$, and eq 19 reduces to

$$k_d = 0 \quad (21)$$

i.e., there is no net desorption of radicals.

Equation 19 unveils some interesting and unexpected features of radical desorption. To illustrate these features, simulations using the parameters given in Table 1 were carried out. Since the model is not restricted to a particular system, these values are not meant to correspond to a given system, but are typical values found in emulsion polymerization. The model predicts

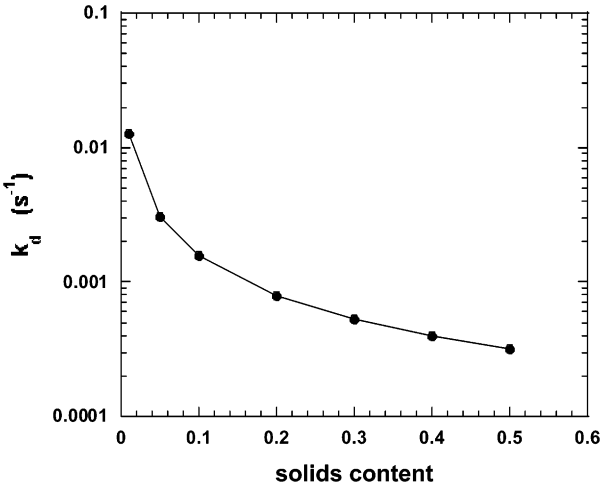

Figure 2. Effect of the solids content on the desorption rate coefficient ($R = 50$ nm).

Table 1. Parameters Used in the Calculations

k_p (L/mol s)	833
k_{tw} (L/mol s)	5×10^9
k_{fm} (L/mol s)	0.017
D_p (dm^2/s)	2×10^{-8}
D_h (dm^2/s)	1×10^{-7}
D_w (dm^2/s)	2×10^{-7}
$[M]_p$ (mol/L)	4.2
$[M]_w$ (mol/L)	0.06
m	70
$[R]_w$ (mol/L)	5×10^{-8}
δ_1 (dm)	5×10^{-8}

that, for a given particle size, the desorption rate coefficient depends on the number of polymer particles, namely, on the solids content. Figure 2 presents the effect of the solids content of the desorption rate coefficient. It can be seen that k_d decreases significantly when the solids content increases. The reason is that the higher the solids constant the more likely it is that the desorbed monomeric radicals reenter the polymer particles and hence the lower the net exit rate. An important practical consequence of this result is that the desorption rate coefficients estimated at low solids contents (conditions frequently used in kinetic studies) cannot be directly used to predict the behavior of a high solids content latex.

Equation 19 also predicts that the rate coefficient for radical desorption increases with the concentration of radicals in the aqueous phase, namely, with the initiator concentration, or by substituting a thermal initiator by a redox system (Figure 3). The reason is that the higher the concentration of radicals in the aqueous phase the less likely is that the desorbed monomeric radicals reenter into the polymer particles, and hence the higher the net exit rate. This means that the use of a value of k_d obtained with a given initiator concentration to predict the behavior of an emulsion polymerization using a different initiator or a different initiator concentration may lead to considerable errors.

Following the pioneering work of Nomura,[7] the desorption rate coefficient is often[13,14] considered to be inversely proportional to the square of the particle diameter. However, the simulations presented in Figure 4 surprisingly show that, for a constant solids content, the radical desorption rate coefficient is not significantly affected by the particle size. The reason is that at constant solids content, a decreasing particle size results in an increase of the number of polymer particles.

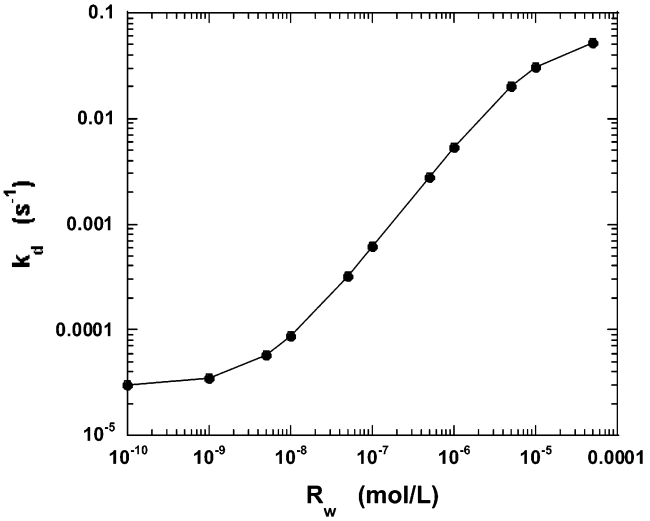

Figure 3. Effect of the concentration of radicals in the aqueous phase on the desorption rate coefficient ($R = 50$ nm, solids content = 50 wt %).

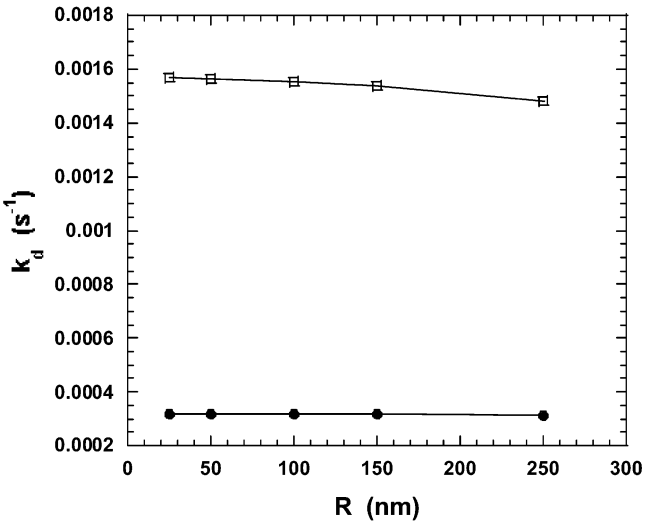

Figure 4. Effect of the particle size on the rate coefficient for radical exit at constant solids contents. Legend: (squares) 10 wt %; (circles) 50 wt %.

Therefore, there are two counteracting effects. On one hand, the smaller the particle size the easier it is for the monomeric radicals to leave the polymer particle. On the other hand, the higher the number of polymer particles the more likely it is that the desorbed radicals reenter the polymer particles.

Figure 5 presents the effect of particle diameter on the desorption rate coefficient for a constant number of polymer particles. It can be seen that k_d severely decreases with the particle size. However, the dependence of k_d with respect to R varies with the particle size.

A consequence of the present model for radical exit is that many of the previous kinetic analysis aiming at estimating k_d must be reevaluated, because in these analysis a single value of k_d was estimated using data obtained with experimental designs in which both the number of polymer particles and the initiator concentration were varied. Under these conditions, eq 19 predicts different values of k_d for the different runs. This may be the reason kinetic analysis based on extensive experimental designs were not conclusive in terms of

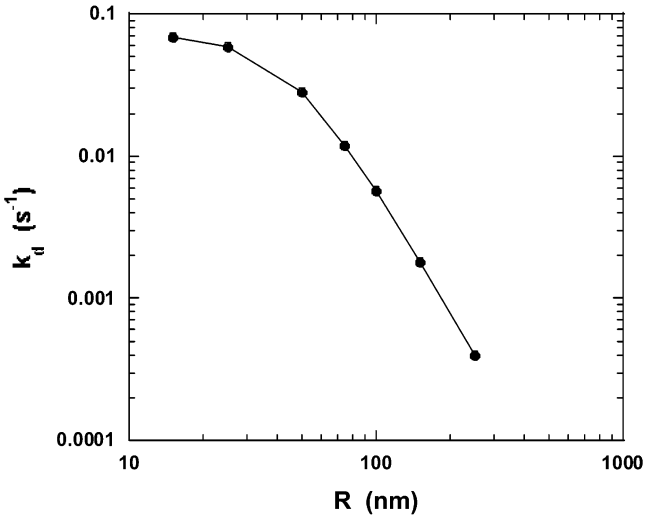

Figure 5. Effect of the particle size on the desorption rate coefficient at constant number of polymer particles ($N_p = 6 \times 10^{15}$ particles/L).

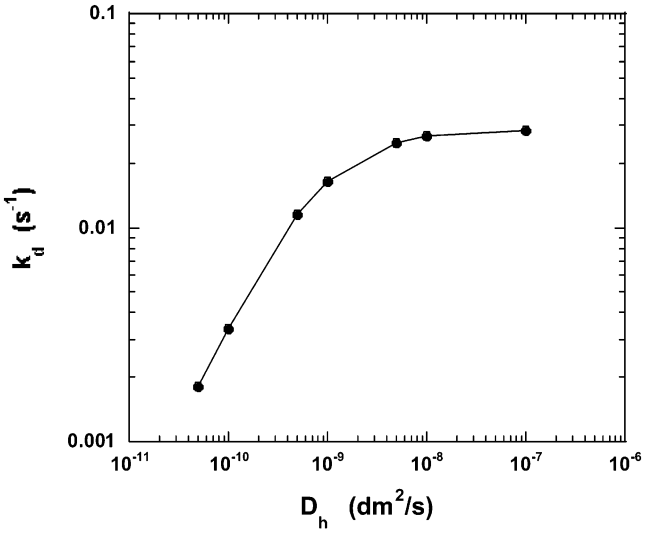

Figure 6. Effect of the resistance offered by the hairy layer on k_d ($R = 50$ nm, $N_p = 6 \times 10^{15}$ particles/L).

the elucidation of the mechanisms involved in radical exit.[15−19]

Coen et al.[20] and Vrowerg and Gilbert[21] reported that the rate of radical desorption severely decreased when a large amount of steric surfactant was used. Figure 6 presents the effect of the resistance of the hairy layer (simulated varying the value of D_h) on the rate coefficient for radical exit. The larger the value of D_h the lower the resistance offered by the hairy layer to the exit of radicals. It can be seen that the present model accounts for the experimental findings.

Conclusions

A new first principles model for radical desorption in emulsion polymerization was developed. There was a need of a new model because the previous models were erroneous. The new model unveils unexpected effects of several operational variables on k_d. In particular, k_d decreases with the number of polymer particles in the system because when N_p increases, it is more likely that the desorbed radicals reenter the polymer particles. On the other hand, k_d increases as the concentration of radicals in the aqueous phase increases, namely, with

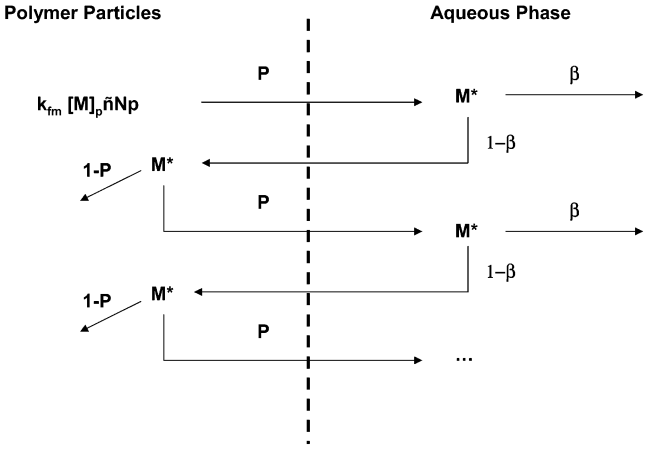

Figure 7. Processes involved in radical desorption.

increasing the initiator concentration or using redox systems. This may be the reason kinetic analysis based on extensive experimental designs were not conclusive in terms of the elucidation of the mechanisms of radical exit. A practical consequence is that the desorption rate coefficients determined under some given experimental conditions cannot be directly used to predict the behavior of emulsion polymerization systems under different conditions.

Another surprising result is that, for constant solids content, k_d was not significantly affected by the particle size because of the counteracting effect of the decreasing particle size and an increasing number of particles. Nevertheless, for a constant number of particles, k_d decreases as particle size increases. The dependence of k_d on particle size varies with the size of the polymer particles. The present model also accounts for the reduction of the radical desorption rate coefficient caused by dense hairy layers.

Appendix I. Approximate Desorption Rate Coefficient

The approach used to derive the desorption rate coefficient given by eq 19 was based on rigorous material balances. In this appendix, an approach somehow similar to those used in the previous models was used to derive an approximate, albeit quite accurate, desorption rate coefficient. Figure 7 illustrates the processes involved in radical desorption. Monomeric radicals are generated by chain transfer to monomer in the polymer particles at a rate equal to $k_{fm}[M]_p \tilde{n} N_p$ (radicals/L·s). These radicals may either react in the polymer particle or desorb from the polymer particle. The probability of desorption, P, is

$$P = \frac{K_o}{K_o + k_p[M]_p} \tag{I-1}$$

where it was assumed that the rate of propagation was much larger than the rate of termination, and in the absence of a hairy layer, the approximate rate of diffusion out of the polymer particle is given by[7]

$$K_o = \frac{3D_w}{R^2 m} \frac{1}{1 + \frac{2D_w}{mD_p}} (s^{-1}) \tag{I-2}$$

Once in the aqueous phase, the monomeric radicals may

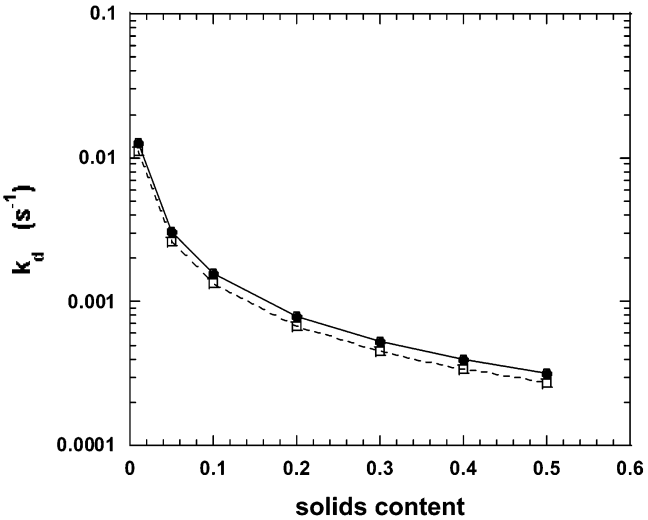

Figure 8. Comparison between the rigorous (circles) and the approximate (squares) radical desorption models ($R = 50$ nm).

react by propagation and termination or may reenter into the polymer particles. The probability of reacting in the aqueous phase is

$$\beta = \frac{k_p[M]_p + k_t[R]_w}{R_{reentry} + k_p[M]_p + k_t[R]_w} \quad \text{(I-3)}$$

In the context of Figure 7 and in the absence of a hairy layer, the rate of reentry is the rate of diffusion of the monomeric radicals through the stagnant stationary layer given by

$$R_{reentry} = 4\pi D_w R(s^{-1}) \quad \text{(I-4)}$$

Under steady-state conditions, the net rate for radical exit is

$$R_{exit} = k_{fm}[M]_p \tilde{n} N_p\{[P + P^2(1-\beta) + P^3(1-\beta)^2 + ...] - [P(1-\beta) + P^2(1-\beta)^2 + ...]\} \text{ (radicals/L·s)} \quad \text{(I-5)}$$

which reduces to

$$R_{exit} = k_{fm}[M]_p \tilde{n} N_p \beta \frac{P}{1 - P(1-\beta)} \text{ (radicals/L·s)} \quad \text{(I-6)}$$

Therefore, the approximate desorption rate coefficient is as follows:

$$k_d = k_{fm}[M]_p \beta \frac{P}{1 - P(1-\beta)} (s^{-1}) \quad \text{(I-7)}$$

When all the desorbed radicals react in the aqueous phase, $\beta = 1$, and eq I-7 approaches eq 2. On the other hand, when the reactions of the desorbed radicals in the aqueous phase are negligible, $\beta = 0$, and in agreement with the rigorous desorption rate coefficient, eq I-7 predicts no desorption of radicals. Figure 8 presents a comparison between the predictions of eqs 19 and I-7. It can be seen that eq I-7 provides a fairly good prediction of k_d. However, it has to be pointed out that the use of the approximate model does not provide any advantage in terms of simplicity or computational efficiency. Therefore, the use of the rigorous model is advised.

Appendix II. Desorption Rate Coefficient in the Presence of Surface Anchoring Effect

Water-soluble initiators are often used in emulsion polymerization. The radicals formed in the aqueous phase from the initiator contain a hydrophilic end, and hence they may be anchored to the surface of the polymer particles. This may lead to a radical concentration profile in the polymer particle. The existence of the radical concentration profiles may affect radical desorption because the probability of generating monomeric radicals near the particle surface increases, and hence the rate of radical exit may increase. Methods for the calculation of these concentration profiles have been given elsewhere,[22,23] and the detailed discussion of this topic is out of the scope of the present article. Nevertheless, it is worth showing how the present model can be adapted to systems in which there is a radical concentration profile.

Let us consider that the radical concentration profile is given by the following equation:

$$[R]_p = \alpha_1\left(1 + \alpha_2\left(\frac{r}{R}\right)^2\right) \quad \text{(II-1)}$$

where α_2 is a parameter defining the steepness of the radical concentration profile and α_1 is proportional to the number of radicals per particle n, according to the following equation obtained integrating the radical concentration profile for the whole particle

$$\alpha_1 = \frac{n}{v_p N_A(1 + 0.6\alpha_2)} \quad \text{(II-2)}$$

The material balance of monomeric radicals in the polymer particles is

$$D_p \frac{1}{r^2}\frac{d\left(r^2 \frac{dC_{M^*}}{dr}\right)}{dr} + k_{fm}[M]_p \frac{n}{v_p N_A(1 + 0.8\alpha_2)} \times \left(1 + \alpha_2\left(\frac{r}{R}\right)^2\right) = k_p[M]_p C_{M^*} \quad \text{(II-3)}$$

where it was considered that propagation was much more likely than termination.

Integration of eq II-3 yields the concentration profile of monomeric radicals, which allows calculating the rate of exit as

$$R_{exit1}(n) = 4\pi R^2 D_p\left(-\frac{dC_{M^*}}{dr}\right)_{r=R} = 4\pi R D_p \times (R\sqrt{\eta}\coth R\sqrt{\eta} - 1)\left[\frac{\Psi n}{\eta} - C_{M^*s}\right] \text{ (mol/s·particle)} \quad \text{(II-4)}$$

where

$$\Psi = \frac{\gamma}{(1 + 0.6\alpha_2)}\left(1 + \alpha_2\left(1 + \frac{6}{R^2\eta} - \frac{2}{R\sqrt{\eta}\coth R\sqrt{\eta} - 1}\right)\right) \quad \text{(II-5)}$$

Equation II-4 is equivalent to eq 9. The rates of exit of

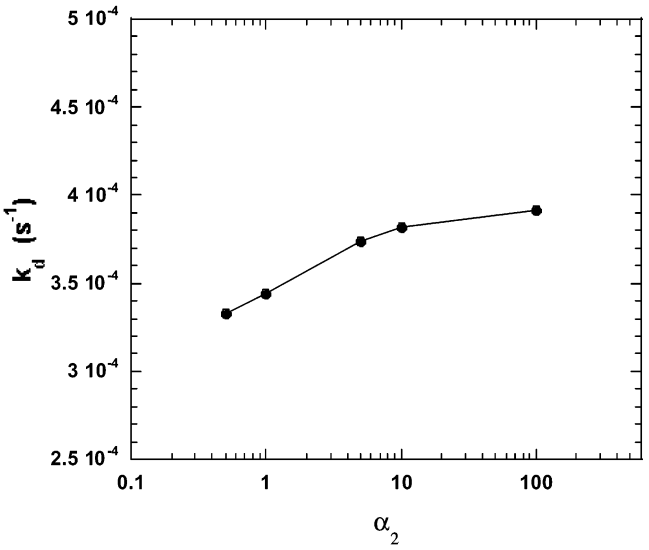

Figure 9. Effect of the surface anchoring on radical desorption ($R = 200$ nm; $D_p = 5 \times 10^{-10}$).

monomeric radicals through the hairy layer and the stationary liquid film are given by eqs 10 and 12. Combination of eqs II-4, 10, and 12 led to the following equation for the desorption rate coefficient:

$$k_d = \lambda \frac{\Psi N_A}{\eta m}\left(1 - \frac{\lambda N_p}{\lambda N_p + k_p[M]_w + 2k_{tw}[R]_w}\right) (s^{-1}) \quad \text{(II-6)}$$

It is worth noticing the similarity between eq II-6 and eq 19 and noticing that when α_2 approaches zero, eq II-6 approaches eq 19. Figure 9 presents the effect of the radicals concentration profile for particles of $R =$ 200 nm. Relatively large particles were used in the simulations because radical concentration profiles are not expected in small particles. It can be seen that the exit rate coefficient significantly increases with the steepness of the radical concentration profile.

Appendix III. Estimation of the Relative Value of δ_2

The rate coefficient for mass transfer through a stationary layer surrounding a spherical particle can be estimated by means of the following equation[24]

$$Sh = 2 + 0.6\{Re\}^{0.5} Sc^{0.33} \quad \text{(III-1)}$$

where Sh is the Sherwood number ($k_g 2R/D_w$), Re the Reynolds number ($2Ru\rho/\mu$), and Sc the Schmidt number ($\mu/\rho D_w$), k_g is the mass transfer rate coefficient, u is the relative velocity between the particle and the aqueous phase, and ρ and μ are the density and viscosity of the aqueous phase, respectively. The latex particles are that small that they move with the fluid, and hence u is close to zero. Consequently, $Sh = 2$, and

$$k_g = \frac{D_w}{R} (dm/s) \quad \text{(III-2)}$$

In terms of the mass transfer rate coefficient, the diffusion of the monomeric radicals through the stationary layer is as follows:

$$R_{exit3} = 4\pi R^2 k_g (C_{M^*h} - C_{M^*w}) (mol/s \cdot particle) \quad \text{(III-3)}$$

Combination of eqs III-2 and III-3 and comparison of the resulting equation with eq 12 yield

$$R = (R + \delta_1)\frac{(R + \delta_1 + \delta_2)}{\delta_2} \quad \text{(III-4)}$$

Because the thickness of the hairy layer is usually much smaller than the particle size, eq III-4 reduces to

$$1 = \frac{(R + \delta_2)}{\delta_2} \quad \text{(III-5)}$$

which yields

$$R \ll \delta_2 \quad \text{(III-6)}$$

Acknowledgment. Financial support from The University of the Basque Country and CICYT (Project PPQ2000-1185) is acknowledged.

References and Notes

(1) Asua, J. M., Ed. *Polymeric Dispersions: Principles and Applications*; Kluwer Academic Press; Dordrecht, The Netherlands, 1997.
(2) Ugelstad, J.; El-Aasser, M. S.; Vanderhoff, J. W. *J. Polym. Sci. Lett. Ed.* **1972**, *11*, 503.
(3) Antonietti, M.; Landfester, K. *Prog. Polym. Sci.* **2002**, *27*, 689.
(4) Asua, J. M. *Prog. Polym. Sci.* **2002**, *27*, 1283.
(5) Qiu, J.; Charleux, B.; Matyjaszewski, K. *Prog. Polym. Sci.* **2001**, *26*, 2083.
(6) Cunningham, M. F. *Prog. Polym. Sci.* **2002**, *27*, 1039.
(7) Nomura, M. In *Emulsion Polymerization*; Piirma, I., Ed.; Academic Press: New York, 1982.
(8) Asua, J. M.; Sudol, E. D.; El-Aasser, M. S. *J. Polym. Sci., Part A: Polym. Chem.* **1989**, *27*, 3909.
(9) Adams, M. E.; Napper, D. H.; Gilbert, R. G.; Sangster, D. F. *J. Chem. Soc., Faraday Trans. 1* **1986**, *82*, 1979.
(10) Casey, B. S.; Morrison, B. R.; Maxwell, I. A.; Gilbert, R. G. *J. Polym. Sci., Part A: Polym. Chem.* **1994**, *32*, 605.
(11) Barandiaran, M. J.; Asua, J. M. *J. Polym. Sci., Part A: Polym. Chem.* **1996**, *34*, 309.
(12) Hansen, F. K.; Ugelstad, J. In *Emulsion Polymerization*; Piirma, I., Ed.; Academic Press: New York, 1982.
(13) Gilbert, R. B. *Emulsion Polymerization. A Mechanistic Approach*; Academic Press: London, U.K., 1995.
(14) Plessis, C.; Arzamendi, G.; Leiza, J. R.; Schoonbrood, H. A. S.; Charmot, D.; Asua, J.M. *Ind. Eng. Chem. Res.* **2001**, *40*, 3883.
(15) Hawkett B. S.; Napper, D. H.; Gilbert R. G. *J. Chem. Soc., Faraday Trans. 1* **1980**, *76*, 1323.
(16) Penboss, I. A.; Gilbert R. G.; Napper D. H. *J. Chem. Soc., Faraday Trans. 1* **1986**, *82*, 2247.
(17) Asua, J. M.; de la Cal, J. C. *J. Appl. Polym. Sci.* **1991**, *42*, 1869.
(18) Barandiaran, M. J.; López de Arbina, L.; de la Cal, J. C.; Gugliotta, L. M.; Asua, J. M. *J. Appl. Polym. Sci.* **1995**, *55*, 1231.
(19) López de Arbina, L.; Barandiaran, M. J.; Gugliotta, L. M.; Asua, J. M. *Polymer* **1996**, *37*, 5907.
(20) Coen, E. M.; Lyons R. A.; Gilbert, R. G. *Macromolecules* **1996**, *29*, 5128.
(21) Vorwerg, L.; Gilbert, R. G. *Macromolecules* **2000**, *33*, 6693.
(22) Chern, C. S.; Poehlein, G. W. *J. Polym. Sci., Polym. Chem. Ed.* **1987**, *25*, 617.
(23) de la Cal, J. C.; Urzay, R.; Zamora, A.; Forcada, J.; Asua, J. M. *J. Polym. Sci., Part A: Polym. Chem.* **1990**, *28*, 1011.
(24) Ranz, W. D.; Marshall, W. R. *J. Chem. Eng. Prog.* **1952**, *48*, 141.

MA0345192